THE JOURNAL OF BIOLOGICAL CHEMISTRY VOL. 292, NO. 6, pp. 2278–2286, February 10, 2017

The Inhibitory Role of α2,6-Sialylation in Adipogenesis*[S]

Received for publication, July 10, 2016, and in revised form, December 17, 2016 Published, JBC Papers in Press, December 28, 2016, DOI 10.1074/jbc.M116.747667

Tomoko Kaburagi[‡§1], **Yasuhiko Kizuka**[§], **Shinobu Kitazume**[§], **and Naoyuki Taniguchi**[§2]

From the [‡]*Department of Health Science, Faculty of Sports and Health Sciences, Daito Bunka University, Higashi-Matsuyama, Saitama 355-8681, Japan and the* [§]*Disease Glycomics Team, Systems Glycobiology Research Group, RIKEN-Max Planck Joint Research Center for Systems Chemical Biology, Global Research Cluster, RIKEN, Wako, Saitama 351-0198, Japan*

Edited by Gerald W. Hart

Adipose tissue plays critical roles in obesity and related diseases such as diabetes and cardiovascular diseases. Previous reports suggest that glycans, the most common posttranslational modifications, are involved in obesity-related diseases, but what type of glycan regulates adipogenesis during obesity remains unclear. In this study, we first quantified the mRNA levels of 167 genes (encoding 144 glycosyltransferases and 23 related enzymes) in visceral adipose tissues (VATs) from control mice and high-fat diet (HFD)-induced obese mice. We found that a gene encoding β-galactoside α2,6-sialyltransferase-1 (*St6gal1*), a key enzyme responsible for the biosynthesis of α2,6-linked sialic acid in *N*-linked glycans, was most down-regulated in VATs from obese mice. We confirmed the reduction in α2,6-sialic acid in VATs from obese mice and differentiated adipocyte model 3T3-L1 cells. Using proteomic analysis, integrin-β1 was identified as one of the target α2,6-sialylated proteins in adipose tissues, and phosphorylation of its downstream molecule focal adhesion kinase was found to be decreased after HFD feeding. *St6gal1* overexpression in differentiating 3T3-L1 cells inhibited adipogenesis with increased phosphorylation of focal adhesion kinase. Furthermore, *St6gal1* knockout mice exhibited increased bodyweight and VAT weight after HFD feeding. The down-regulation of *St6gal1* during adipogenesis was canceled by treatment with a DNA methyltransferase inhibitor, suggesting an involvement of epigenetic DNA methylation in *St6gal1* silencing. Our findings suggest that ST6GAL1 has an inhibitory role in adipogenesis through integrin-β1 activation, providing new insights into the roles and regulation mechanisms of glycans in adipocytes during obesity.

Currently, adipose tissue is recognized as an endocrine organ that controls metabolism-related diseases (1, 2). Adipocytokines, which are bioactive molecules secreted from adipose tissue, are involved in energy metabolism, vascular homeostasis, and the immune response (1–5). Obesity results from excess accumulation of adipose tissue with hypertrophy and hyperplasia of adipocytes (5–9), which leads to abnormal secretion of adipocytokines (6, 7) and triggers various diseases, including diabetes and cardiovascular diseases (2, 6, 7, 10). Although these morphofunctional modifications of adipocyte are related to cell adhesion molecules, such as integrins (11, 12), the precise molecular mechanisms behind the adipocyte growth (referred to as adipogenesis) in obesity are not fully understood.

Glycosylation is the most common posttranslational modification of proteins and confers both structural and functional diversity to proteins (13, 14). The biosynthesis of glycans is catalyzed by glycosyltransferases, and ~200 glycosyltransferases have been cloned in mammals (13, 15, 16). The development of various diseases, including diabetes, cardiovascular diseases, and emphysema, is regulated by glycosylation via the action of glycosyltransferases (17–22). Considering that these disorders are closely related to obesity, their product glycans are also assumed to be involved in the dysfunction of adipose tissue by obesity.

There are now some reports showing that obesity functionally changes the expression of glycans in adipose tissues. Ganglioside GM3 is up-regulated in adipose tissue by obesity, which leads to insulin resistance (19, 20). It is also reported that, in the 3T3-L1 adipocyte cell model, *O*-GlcNAcylation and *N*-glycosylation are involved in adipogenesis or adipocyte differentiation and insulin-induced uptake of glucose (23–26). These findings strongly suggest that glycosylation in adipose tissue is also key to understanding the molecular mechanisms underlying obesity and related diseases. However, it is not fully understood which glycans are functionally involved in adipogenesis during obesity.

In this study, we used a mouse model of high fat diet (HFD)-induced[3] obesity and adipocyte model 3T3-L1 cells to identify glycosyltransferase genes whose expression was altered in visceral adipose tissues (VATs) during obesity. We found that β-galactoside α2,6-sialyltransferase-1 (ST6GAL1), a key enzyme responsible for the formation of the Siaα2,6-Gal linkage in *N*-linked glycans, was the most down-regulated glycosyltransferase in VATs from obese mice compared with control

* This work was supported by RIKEN (the Systems Glycobiology Research Project) (to N. T.) and by Japan Society for the Promotion of Science Grant-in-Aid for Challenging Exploratory Research 15K14481 (to N. T.), Grant-in-Aid for Scientific Research (B) 15H04700 (to N. T.), and Grant-in-Aid for Scientific Research (C) 15K00885 (to T. K.). The authors declare that they have no conflicts of interest with the contents of this article.

[S] This article contains supplemental Figs. 1–4.

[1] To whom correspondence may be addressed: Dept. of Health Science, Faculty of Sports and Health Sciences, Daito Bunka University, 560 Iwadono, Higashi-matsuyama, Saitama, Japan. Tel.: 81-493-31-1558; Fax: 81-493-31-1562; E-mail: t-kabu@ic.daito.ac.jp.

[2] To whom correspondence may be addressed: Disease Glycomics Team, Systems Glycobiology Research Group, RIKEN-Max Planck Joint Research Center for Systems Chemical Biology, Global Research Cluster, RIKEN, 2-1 Hirosawa, Wako, Saitama, Japan. Tel.: 81-48-467-9616; Fax: 81-48-467-9617; E-mail: dglycotani@riken.jp.

[3] The abbreviations used are: HFD, high-fat diet; VAT, visceral adipose tissue; CON, control; SSA, *Sambucus sieboldiana* agglutinin; FAK, focal adhesion kinase; 5-AZA, 5-aza-2′-deoxycytidine; C/EBP, CCAAT enhancer-binding protein.

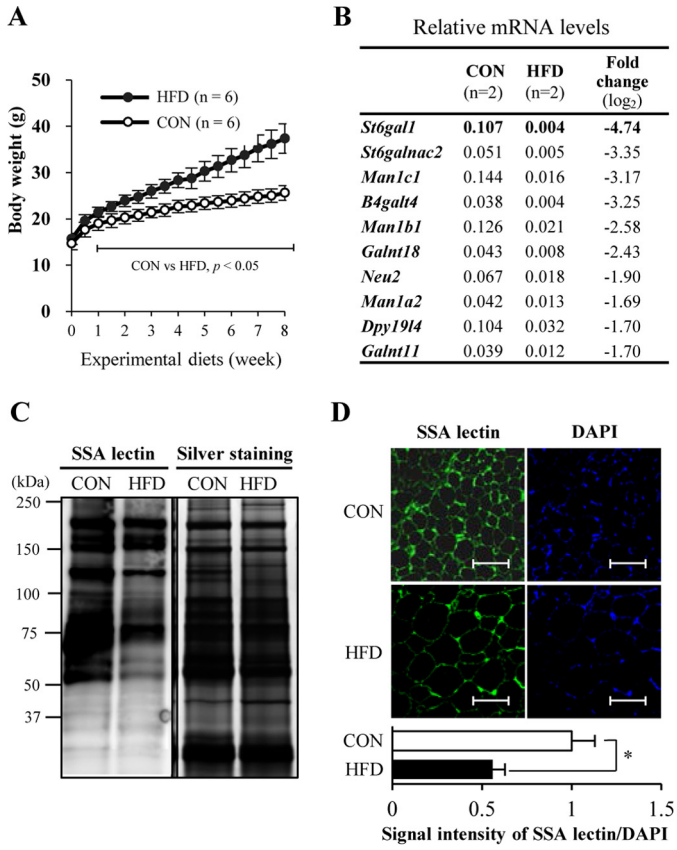

	CON (n=2)	HFD (n=2)	Fold change (log_2)
St6gal1	**0.107**	**0.004**	**-4.74**
St6galnac2	0.051	0.005	-3.35
Man1c1	0.144	0.016	-3.17
B4galt4	0.038	0.004	-3.25
Man1b1	0.126	0.021	-2.58
Galnt18	0.043	0.008	-2.43
Neu2	0.067	0.018	-1.90
Man1a2	0.042	0.013	-1.69
Dpy19l4	0.104	0.032	-1.70
Galnt11	0.039	0.012	-1.70

FIGURE 1. **St6gal1 is the most down-regulated glycosyltransferase gene in VATs of obese mice.** *A*, change in body weight of C57BL6/J male mice fed a CON diet ($n = 6$) or HFD ($n = 6$). *B*, the top 10 down-regulated glycosyltransferase and related enzyme genes in VATs of HFD mice ($n = 2$). *C*, proteins extracted from mouse VATs were subjected to SDS-PAGE, transferred onto a nitrocellulose membrane, and stained with SSA lectin. Proteins in the gel were also silver-stained after SDS-PAGE. *D*, lectin fluorescence staining for α2,6-sialylated proteins. Mouse VATs were stained with SSA lectin (*green*). *Scale bar* = 100 μm. Nuclei were counterstained with DAPI (*blue*). Fluorescence intensity relative to that of CON samples was quantified ($n = 3$). All graphs show means ± S.E. (*, $p < 0.05$; **, $p < 0.01$; Student's *t* test).

(CON) mice fed a normal diet. We also showed that ST6GAL1-mediated α2,6-sialylation of integrin-β1 is one of the negative factors in adipogenesis. Furthermore, *St6gal1* knockout mice exhibited increased body weight and VAT weight. These results underscore a novel role for protein sialylation in obesity.

Results

St6gal1 Is the Most Down-regulated Glycosyltransferase Gene in VATs of HFD Mice—To investigate how glycosylation is involved in obesity, we first designed experiments using HFD-fed obese mice. HFDs induce obesity in mice with dysregulated metabolism of glucose and lipid as well as disturbed production of adipocytokines (4, 9, 27, 28). We confirmed that body weights were heavier in our HFD mice than in CON mice after 8 weeks on the experimental diets (Fig. 1*A*). We then quantified the mRNA levels of 167 genes (encoding 144 glycosyltransferases and 23 related enzymes, covering most of the glycosyltransferases identified to date) in VATs from CON and HFD mice (supplemental Figs. 1 and 2). The top nine most highly expressed genes in VATs from CON mice (with expression levels >0.1 of those of the housekeeping genes) are shown in supplemental Fig. 3. Using a previous quantitative PCR study of other mouse tissues (brain, liver, testis, and kidney) for comparison (29), VAT expresses a unique set of glycan-related genes. For example, the VAT shows high levels of *B3galt2* and undetectable levels of *B3gnt2* and *A3galt2*, which are highly expressed in other tissues (supplemental Figs. 1–3) (29), demonstrating tissue-specific regulation of glycan expression. Compared with VATs from CON mice, limited numbers of genes were found to be up-regulated in VATs from HFD mice (supplemental Figs. 1 and 2). But, more strikingly, several genes were dramatically down-regulated in VATs from HFD mice (Fig. 1*B* and supplemental Figs. 1 and 2). *St6gal1* was the most down-regulated gene, reduced to less than 4% of CON levels, suggesting that ST6GAL1 has roles in visceral adipocytes. We further confirmed a reduction in the amount of ST6GAL1 products (namely, α2,6-sialic acid) in mouse VATs by both lectin blotting (Fig. 1*C*) and histochemical staining (Fig. 1*D*), with *Sambucus sieboldiana* agglutinin (SSA) lectin, which specifically recognizes α2,6-sialylated glycoconjugates (30). The morphology of adipocytes with large lipid droplets and its hypertrophic change by HFD feeding are consistent with other previous reports (31, 32).

Integrin-β1 Was Identified as an α2,6-Sialylated Protein in Mouse VATs by Mass Spectrometry—To elucidate the mechanisms by which ST6GAL1-mediated protein sialylation is involved in obesity, we set out to identify the target protein functionally modified by ST6GAL1 in adipose tissues. We biochemically purified the α2,6-sialylated proteins in VATs using SSA lectin. As shown in Fig. 2*A*, of several proteins with reduced reactivity to SSA, a protein of 120–130 kDa showed a clear reduction in SSA reactivity under HFD feeding (*arrow*), whereas many other proteins showed no changes. A reduction in SSA reactivity of the 120- to 130-kDa protein was also observed with lectin blotting, as shown in Fig. 1*C*. We excised this 120- to 130-kDa band and, using MS analysis, identified six candidate proteins to be included (Fig. 2*B* and supplemental Fig. 4). We focused on integrin-β1 because its molecular weight was consistent with the band, and previous studies report that integrins are involved in adipocyte differentiation (33–35). We found that α2,6-sialylation of integrin-β1 in mouse VATs was significantly reduced in HFD mice compared with CON mice (Fig. 2*C*). The loss of SSA reactivity of integrin-β1 from *St6gal1* knockout VATs confirmed the specificity of this lectin. To examine the role of α2,6-sialylation on integrin-β1 in adipose tissue, we analyzed phosphorylation of focal adhesion kinase (FAK). FAK is the major downstream regulator of integrin-β1 and is activated by phosphorylation upon binding of integrin-β1 to extracellular matrix proteins such as fibronectin (36, 37). We observed a significant decrease in the phosphorylation levels of FAK in VATs of HFD mice compared with CON mice (Fig. 2*D*). These results indicate that the functions of integrin-β1 in VATs are disturbed during the induction of obesity by HFD feeding, concomitant with the decrease in its α2,6-sialylation.

Down-regulation of St6gal1 in Differentiated 3T3-L1 Adipocytes—Next, using 3T3-L1 cells as a mouse preadipocyte model, we asked whether the expression of *St6gal1* is also down-regulated during adipocyte differentiation. For differentiation, 3T3-L1 cells were treated with dexamethasone,

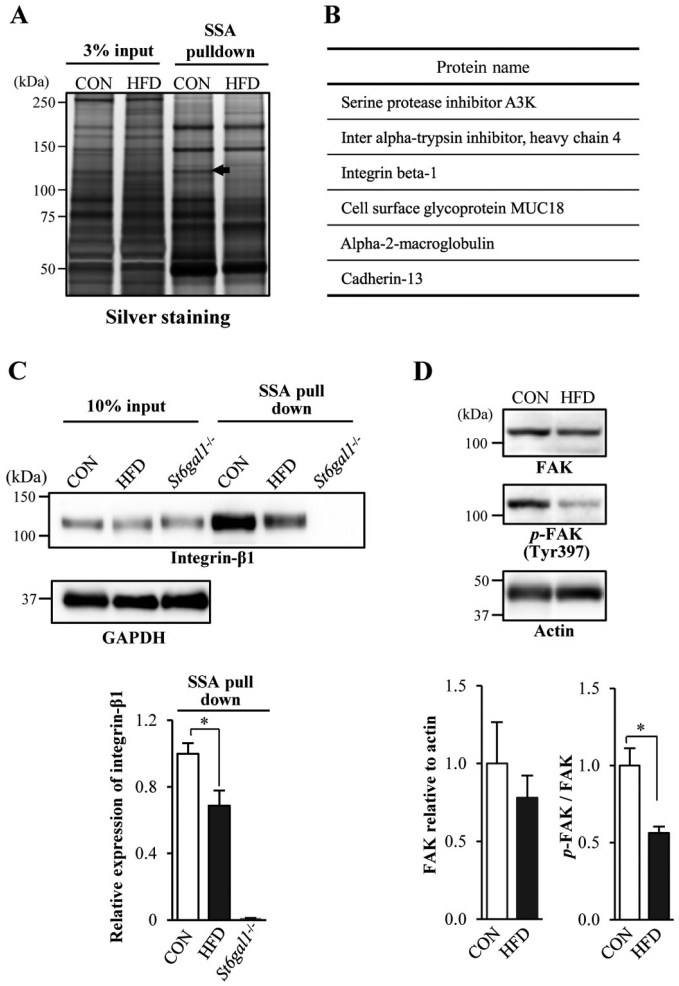

FIGURE 2. **Identification of α2,6-sialylated proteins reduced in VATs from obese mice.** *A*, α2,6-sialylated proteins were pulled down with SSA lectin from mouse VATs and then subjected to SDS-PAGE and silver staining. A precipitated protein (*arrow*, 120–130 kDa) from CON mice that was reduced in HFD-induced obese mice was further analyzed. *B*, proteins (excised from the 120–130-kDa band) identified by MS. *C*, proteins extracted from mouse VATs (*input*) and then pulled down with SSA lectin (*SSA pulldown*) were blotted with anti-integrin-β1 antibody or anti-GAPDH antibody ($n = 3$). *D*, proteins in VATs from CON or HFD mice were blotted with an anti-FAK, anti-phospho-FAK (*p-FAK*), or anti-actin antibody ($n = 3$). The signal intensity of the bands in the Western blot was quantified and is shown as a graph. All graphs show mean ± S.E. (*, $p < 0.05$ by Student's *t* test).

3-isobutyl-1-methylxanthine, and insulin for 2 days, followed by insulin for 12 days according to an established method (38, 39) (Fig. 3*A*, *top panel*). We successfully induced adipocyte differentiation using these cells. This was evidenced by an increased number and enlargement of lipid droplets (Fig. 3*A*, *bottom panel*) and the induction of several key marker genes, including adiponectin (*Adipoq*), peroxisome proliferator-activated receptor γ (*Pparg*), and fatty acid binding protein 4 (*Fabp4*) (Fig. 3*B*). In contrast, the expression level of *St6gal1* was significantly reduced during adipocyte differentiation (Fig. 3*B*), consistent with its down-regulation in the VATs of HFD mice described above.

To explore the transcriptional mechanism underlying the down-regulation of *St6gal1*, we focused on DNA methylation, as adipogenesis is regulated by epigenetic DNA methylation (40, 41). As expected, methylation-specific PCR using the 3T3-L1 genome revealed that methylation in a CpG island of the *St6gal1* promoter was enhanced during adipogenesis (Fig. 3*C*). This suggests that epigenetic DNA hypermethylation is involved in the down-regulation of *St6gal1* expression during adipogenesis. Consistent with this, treatment with a DNA methyltransferase inhibitor, 5-aza-2′-deoxycytidine (5-AZA) canceled the down-regulation of *St6gal1* during adipocyte differentiation (Fig. 3*D*). Considering its down-regulation in both the VATs from HFD mice and 3T3-L1 adipocytes, we hypothesized that ST6GAL1 plays an inhibitory role in adipogenesis.

Overexpression of St6gal1 Inhibited Adipogenesis and Activated Integrin-β1 Signaling—To directly examine whether *St6gal1* expression inhibits adipogenesis, *St6gal1* was overexpressed in 3T3-L1 cells using an adenoviral vector (Fig. 4*A*). As a result, lipid accumulation (as assessed by oil red O staining) was clearly inhibited by overexpression of *St6gal1* (Fig. 4*A*, *bottom panel*). Unexpectedly, however, the markers of adipogenesis showed only a slight decrease in expression with *St6gal1* overexpression (Fig. 4*B*). Adipocyte differentiation generally involves several distinct phases, including proliferation and subsequent growth arrest of preadipocytes as the initial stage, followed by mitotic clonal expansion and terminal differentiation (38, 39). Overexpression of *St6gal1* significantly suppressed preadipocyte proliferation, particularly at the early stage (Fig. 4*C*). Our results suggest that α2,6-sialylation inhibits the early stage of preadipocyte proliferation.

We identified integrin-β1 as a target protein of ST6GAL1 in adipose tissue (Fig. 2) and confirmed that *St6gal1* overexpression increased α2,6-sialylation of integrin-β1 in this cell model (Fig. 4*D*). Integrin-β1 regulates adipocyte differentiation through the downstream activator FAK (34, 36, 42). We found that phosphorylation of FAK was increased by *St6gal1* overexpression in differentiating 3T3-L1 cells (Fig. 4*E*). In addition, the effects of *St6gal1* overexpression on *Cebpb* expression were attenuated by knocking down integrin-β1 (Fig. 4, *F* and *G*), supporting the notion that α2,6-sialylation of integrin-β1 regulates adipogenesis. Collectively, these results suggest that sustained α2,6-sialylation of integrin-β1 suppresses adipogenesis, probably by inhibiting preadipocyte proliferation.

HFD-fed St6gal1 Knockout Mice Gained More Body Weight and VAT Weight—Finally, we analyzed *St6gal1* knockout mice to further investigate the *in vivo* role of ST6GAL1 in adipogenesis. After 8 weeks of HFD feeding, although no significant differences were observed in serum biomarkers (Fig. 5*A*), *St6gal1* knockout mice gained more body weight and VAT weight than littermate heterozygous mice (Fig. 5, *B* and *C*). Intake of energy from the HFD in *St6gal1* knockout mice (17.6 ± 1.0 kcal/mouse/day) was not significantly different from that of the heterozygous mice (15.3 ± 0.7 kcal/mouse/day). The expression level of a proliferation marker, *Ki67* (43), was higher in VAT of *St6gal1* knockout mice than in heterozygous mice (Fig. 6*D*), consistent with results from 3T3-L1 cells, where *St6gal1* overexpression suppressed proliferation of adipocytes. These results indicate that dysregulated adipogenesis, but not excess food intake, in *St6gal1* knockout mice leads to the increase in

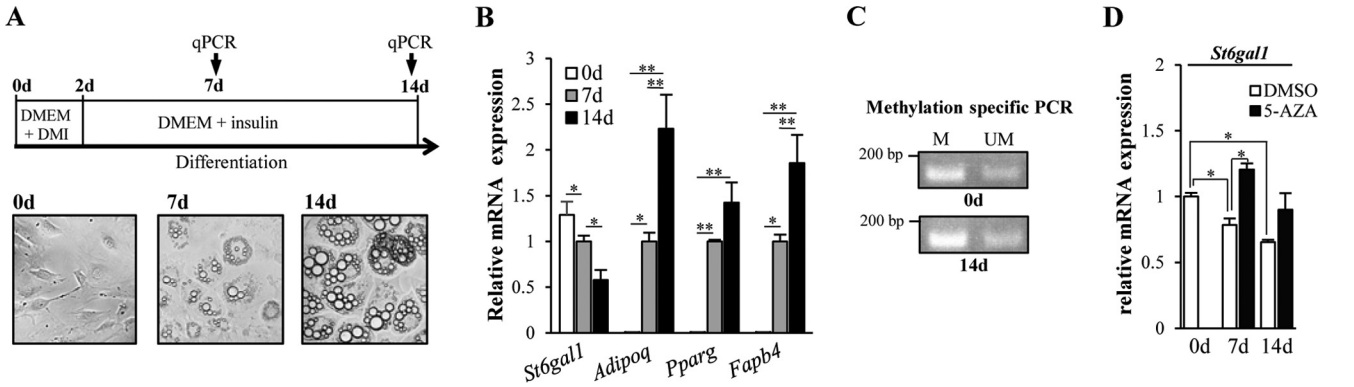

FIGURE 3. **Epigenetic down-regulation of *St6gal1* in differentiated 3T3-L1 adipocytes.** *A*, 3T3-L1 preadipocytes were cultured in DMEM supplemented with dexamethasone, 3-isobutyl-1-methylxanthine, and insulin. 2 days (*d*) post-differentiation (day 2), the medium was replaced with DMEM containing insulin. Over the next 12 days, the medium was replaced every other day with a new one (DMEM containing insulin) (*top panel*). Shown are microscopy images of 3T3-L1 preadipocytes 2 days post-confluence (*bottom panel*, *left*, *0d*), cells 7 days after induction of differentiation (*bottom panel*, *center*, *7d*), and cells 14 days after differentiation (*bottom panel*, *right*, *14d*). *qPCR*, quantitative PCR. *B*, mRNA levels of adipogenesis-related genes in 3T3-L1 cells. *C*, methylation status of the CpG island in the *St6gal1* promoter in differentiated (*14d*) or undifferentiated (*0d*) 3T3-L1 cells. A genomic region in the CpG island was amplified with primers designed for either methylated (*M*) or unmethylated (*UM*) CpG sites. *D*, 5-AZA ($n = 3$) or DMSO ($n = 3$) was added to 3T3-L1 cells every 2 days (days 0, 2, 4, 6, 8, 10, and 12). On days 7 and 14, cells were collected, and the expression level of the *St6gal1* gene was quantified. All graphs show mean ± S.E. (*, $p < 0.05$; **, $p < 0.01$; Tukey's post hoc test).

VAT weight, again suggesting that ST6GAL1 has a suppressive role in obesity.

Discussion

Here we have demonstrated for the first time that α2,6-sialylation inhibits adipogenesis, probably through functional modification of integrin-β1 (Fig. 6). A key glycosyltransferase gene, *St6gal1*, was down-regulated in adipose tissues from obese mice, probably by an epigenetic mechanism. Our results highlight the importance of glycosylation in obesity, which could lead to the development of a novel glycan-targeted strategy for the therapy of obesity-related diseases.

Integrin-β1 is functionally modified by ST6GAL1 (44–47). Previous reports have shown that integrin-β1 regulates various biological functions, including cell migration and signal transduction, and that these functions are partially mediated by its sialylation (44–48). *St6gal1*-null tumors showed a more differentiated phenotype and decreased FAK phosphorylation (49), indicating that ST6GAL1 alters cell properties through its modulation of integrin function, particularly in the context of cancer (50). Furthermore, the activity of integrin-β1 is proposed to be impaired during adipogenesis (12). Adipocyte differentiation is regulated by the downstream signaling of integrin-β1 such as FAK and ERK (34, 36, 42, 51). Consistent with these reports, our *in vivo* and *in vitro* results suggest that reduction of α2,6-sialylation of integrin-β1 is a key event for signaling in adipogenesis. Intriguingly, reduction in α2,6-siaylation seems to be protein-specific (Figs. 1*C* and 2*A*). Although sialylation of some proteins, including integrin-β1, was highly susceptible to *St6gal1* down-regulation, other proteins retained their reactivity to SSA. Determining the mechanisms behind such protein selectivity on glycan alteration is crucial to understanding the detailed functions of glycosylation.

In general, adipogenesis consists of several distinct phases. Differentiation of 3T3-L1 cells into adipocytes also involves several steps (38, 39): an initial proliferation and subsequent growth arrest of preadipocytes, mitotic clonal expansion, and terminal differentiation. This process is regulated by several transcription factors, including peroxisome proliferator-activated receptor γ and CCAAT/enhancer binding proteins (C/EBPβ, C/EBPγ, and C/EBPα). This study shows that the initial preadipocyte proliferation, a prerequisite for subsequent differentiation (52), was inhibited by overexpression of *St6gal1* (Fig. 4*C*). In addition, *St6gal1* overexpression tended to reduce mRNA expression of the key transcription factors, especially *Cebpb* (Fig. 4*B*). Because previous reports indicate that C/EBPβ is required for mitotic clonal expansion (12, 53), ST6GAL1 might also inhibit the clonal expansion step. Although overexpression of *St6gal1* greatly suppressed proliferation of preadipocytes (to approximately 50% of the control) (Fig. 4*C*), decreases in lipid accumulation (Fig. 4*A*) and the differentiation markers (Fig. 4*B*) were modest, suggesting that another unknown mechanism exists by which α2,6-sialylation is involved in regulation of adipogenesis. It should be noted that adipocyte differentiation involves multiple steps and that several glycoproteins were α2,6-sialylated in addition to integrin-β1 (*e.g.* cadherin-13) (Fig. 2, *A* and *B*). We showed that integrin-β1 is one of the functional targets of ST6GAL1 in adipocytes, but the functions of other α2,6-sialylated proteins in adipocytes will need to be determined in the future.

Our results showed that epigenetic DNA hypermethylation is involved in the down-regulation of *St6gal1* expression during adipogenesis (Fig. 3, *C* and *D*). Although little is known about the epigenetic mechanisms governing glycosyltransferase expression (54–56), recent reports have revealed that DNA methylation in the CpG island of glycosyltransferase promoters is involved in their down-regulation, particularly under disease conditions (57). In terms of cancer biology, several mechanisms of epigenetic silencing of the *St6gal1* gene have been reported, mediated by DNA methylation or microRNA (58–60). A more detailed analysis of the pathological regulation of the *St6gal1* gene in adipocytes will be needed in the future.

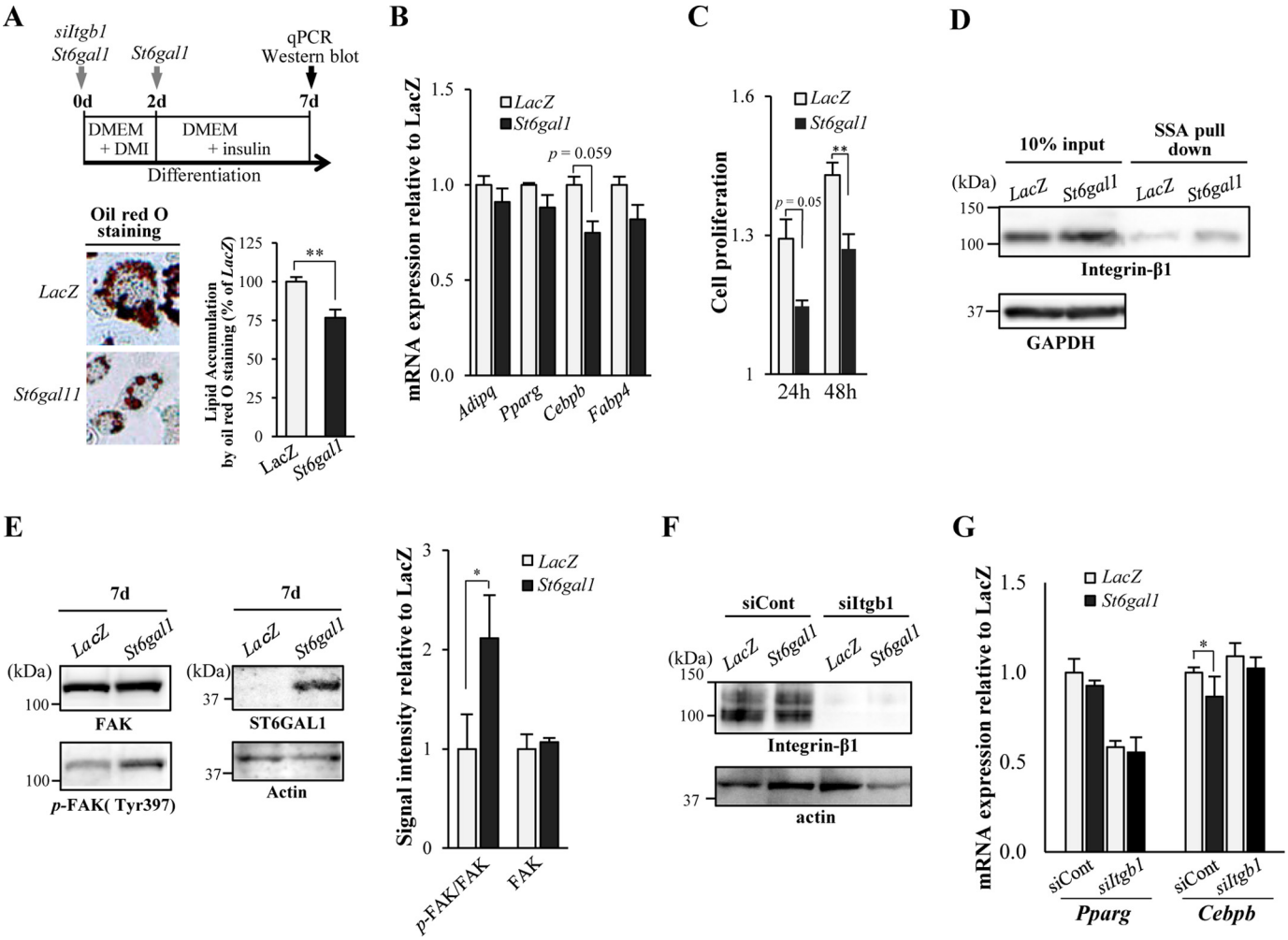

FIGURE 4. **Overexpression of *St6gal1* inhibited adipogenesis and enhanced integrin-β1 activity.** *A*, 3T3-L1 cells were infected with either an adenovirus vector encoding *St6gal1* or a control vector (LacZ) before and during differentiation (days (*d*) 0 and 2), and were transfected with siRNA for *Itgb1* before differentiation (day 0) (*top panel*). Microscopy images of oil red O staining of cells (*bottom panel*, *left*) were taken, and the amount of stained lipid in adipocytes was measured 7 days after differentiation (*bottom panel*, *right*). *qPCR*, quantitative PCR. *B*, on day 7, the levels of mRNA expression of adipogenesis-related genes were quantified ($n = 3$). *C*, 3T3-L1 cells (preadipocytes) were infected with *St6gal1* or a control adenoviral vector (LacZ) on day 0. Cell proliferation was assessed at each time point after induction of differentiation (24 and 48 h) relative to the value of 0 h using the alamarBlue assay ($n = 6$). *D*, α2,6-sialylated proteins were pulled down with SSA lectin from 3T3-L1 lysates on day 7 and then subjected to SDS-PAGE and Western blot for integrin-β1. *E*, lysates of 3T3-L1 adipocytes on day 7 were blotted for FAK, phospho-FAK (*p-FAK*) and ST6GAL1 (*left panel*). The signal intensity of the bands in the Western blot was quantified and is shown as a graph (*right panel*). *F*, 3T3-L1 adipocytes were transfected with control siRNA or siRNA for *Itgb1*. Lysates of the cells on day 7 were blotted for integrin-β1 or actin. *G*, the levels of mRNA expression of adipogenesis-related genes were quantified on day 7 ($n = 3$). All graphs show mean ± S.E. (*, $p < 0.05$; **, $p < 0.01$; Student's *t* test).

St6gal1 knockout mice gained more body weight and VAT weight from HFD feeding than littermate heterozygous mice (Fig. 5, *B* and *C*) with increasing adipocyte proliferation (Fig. 5*D*), suggesting that adipogenesis is abnormally enhanced in these mutant mice. *St6gal1* knockout mice have been reported to show multiple phenotypes involving abnormal B cell responses (61), altered T cell development in the thymus (62), and vulnerability of endothelial cells to apoptotic stimuli (63), but the effects of *St6gal1* deficiency on adipogenesis have not yet been investigated. It was reported previously that SNPs at the *St6gal1* gene are associated with obesity and type 2 diabetes (64, 65). These findings, together with our results, suggest that ST6GAL1 is involved not only in adipogenesis but also in the subsequent development of obesity and related disorders. Although we still do not fully understand the detailed molecular mechanisms of how ST6GAL1 in VAT suppresses adipogenesis, this study provides new insights into the roles of glycans in adipogenesis, which we believe hold potential for a novel therapeutic target for suppressing obesity and its related diseases.

Experimental Procedures

Materials—The following antibodies were used: anti-integrin-β1 (610467) from BD Biosciences, anti-GAPDH (MAB374) and anti-FAK (06-534) from Millipore, anti-phospho-FAK (Tyr-397) (3283) from Cell Signaling Technology, anti-actin (A4700) from Sigma, and anti-ST6GAL1 from Immuno-Biological Laboratories (M2 rabbit polyclonal antibody) (66). Biotinylated SSA lectin was purchased from Seikagaku Corp. Primer-probe sets for mRNA quantification were purchased from Life Technologies: control *Gapdh*, 4308313; ribosomal RNA, 4308329; *St6gal1*, Mm00486119_m1; *Adipoq*, Mm00456425_m1; *Pparg*, Mm00440940_m1; *Fabp4*, Mm00445878_m1; *Cebpβ*, Mm00843434_s1; and *Mki67*, Mm01278617_m1.

siRNAs were purchased from Qiagen: control siRNA, 1027280; mouse *Itgb1*, SI00194026.

Animals and Diets—Male C57BL/6J mice were obtained from Oriental Yeast (Tokyo, Japan). The generation of *St6gal1*-deficient mice has been described previously (61), from a C57BL/6 genetic background. C57BL/6J mice at 6 weeks of age were acclimated with a control diet based on AIN 93G (CON, containing 7% fat, D10012G, Research Diets Inc.) for 1 week. Then mice were fed with an HFD containing 56% fat supplemented with lard (D12052803, Research Diets Inc., $n = 6$) for 8 weeks to induce obesity or fed with a CON ($n = 6$). Littermates, *St6gal1* homozygous (*St6gal1*$^{-/-}$, $n = 4$), and heterozygous knockout mice (*St6gal1*$^{+/-}$, $n = 3$), were given the CON diet for 4 weeks, followed by the HFD for 8 weeks. All mice were allowed free access to water and food. For the period of the study, body weight and food consumption were measured once a week. Prior to sacrifice, blood was collected under anesthesia, and VATs of the epididymis were collected, weighed, and frozen. All mice were housed (three or fewer mice per cage) at 23 ± 3 °C and 55 ± 10% humidity. The light conditions were 14 h:10 h (lights on at 7 a.m.). The Animal Experiment Committee of RIKEN approved all animal experiments.

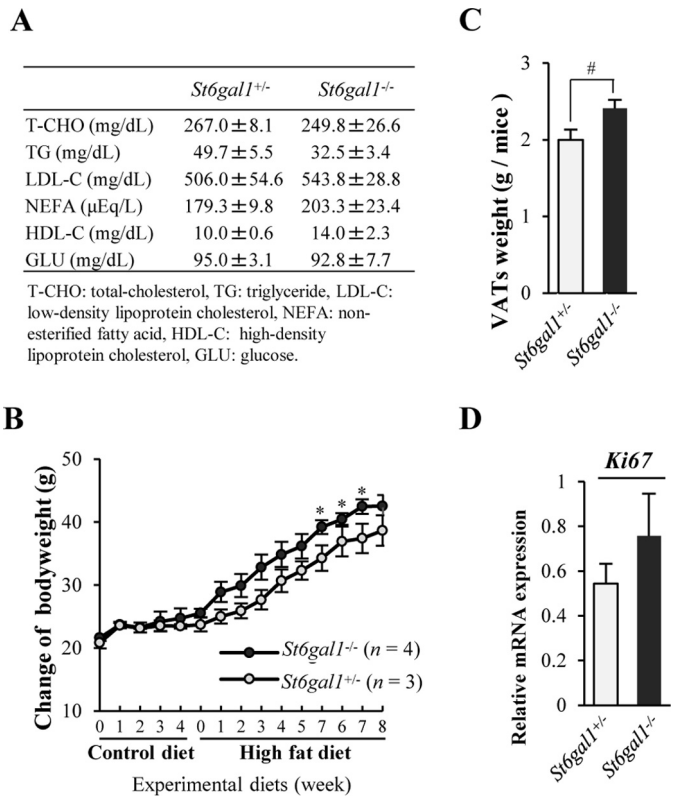

FIGURE 5. **Male *St6gal1* knockout mice gained more body weight and VAT weight from HFD feeding than littermate heterozygous mice.** *A*, levels of serum biochemical markers after 8 weeks of HFD feeding. *B*, change in bodyweight of male mice fed a control diet for 4 weeks and subsequently fed an HFD for 8 weeks. *C*, weight of VATs after 8 weeks of HFD feeding. *D*, mRNA expression of the *Ki67* gene in VATs. All graphs show mean ± S.E. (*, $p < 0.05$ *versus* *St6gal1*$^{+/-}$ by Mann-Whitney *U* test; #, $p < 0.05$ by Student's *t* test).

Real-time PCR for a Large Set of Glycosyltransferase Genes—Specific primers for 144 glycosyltransferase mRNAs and 23 mRNAs for related proteins were purchased from Qiagen in a 96-well-based form (67). Selected genes are listed in supplemental Figs. 1 and 2. Glycosyltransferases responsible for the early steps of *N*-glycan biosynthesis or glycosylphosphatidylinositol synthesis, such as the *Alg* genes, are not included in this list. Total RNA (1 μg) was reverse-transcribed using the RT^2 First Strand Kit (Qiagen) in a 40-μl reaction mixture and then diluted with 182 μl of RNase-free water. The resultant cDNA solution was mixed with 2.7 ml of RT^2 SYBR Green qPCR Mastermix (Qiagen) and 2.496 ml of water, and 25 μl of the mixture was applied to each well. cDNAs were amplified and analyzed using ABI Prism 7900HT (Applied Biosystems), in accordance with the RT^2 Profiler PCR Array Handbook (Qiagen). The abundance of glycosyltransferase mRNA relative to that of housekeeping genes (average of *Actb*, *B2m*, *Gapdh*, and *Hsp90ab1*) was calculated using the ΔCt method.

Protein Extraction from VATs—Mouse VATs were homogenized with TBS containing 1% Triton X-100, a protease inhibitor mixture, and phosphatase inhibitors (Roche Applied Science). The insoluble debris and thick lipid layer were removed after centrifugation at 3000 × *g* for 5 min, and then the lysate

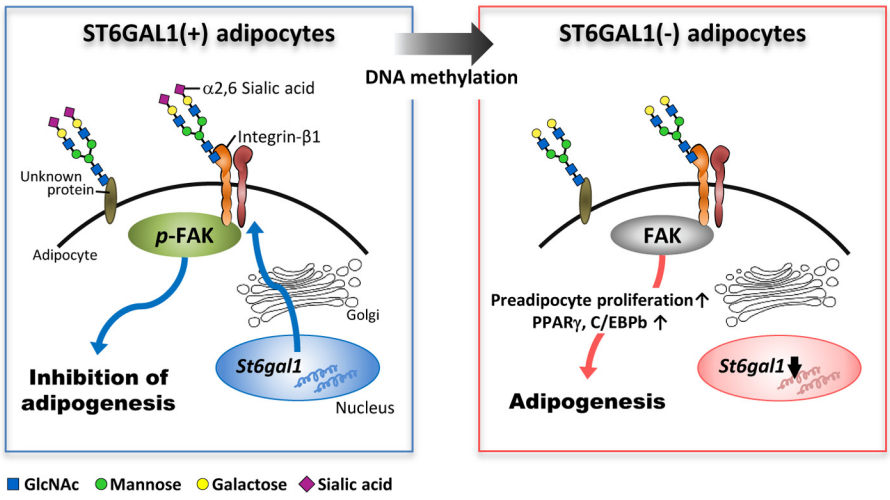

FIGURE 6. **Schematic of the inhibitory role of ST6GAL1 in adipogenesis.** In the presence of ST6GAL1, adipogenesis is inhibited by α2,6-sialylation of integrin-β1 and by activation of downstream signaling, including FAK phosphorylation. During adipogenesis, *St6gal1* expression is epigenetically silenced by DNA methylation, which leads to hyposialylation of integrin-β1, impairment of downstream signaling, and up-regulation of key adipogenic genes.

was sonicated for 5 s. Protein concentrations in tissue extracts and cells were measured using the BCA assay.

Cell Culture, Viral Infection, and siRNA Transfection—The culture procedure for 3T3-L1 cells is shown in brief in Fig. 3*A*. 3T3-L1 preadipocytes were cultured in DMEM supplemented with 10% FBS. 2 days post-confluence (day 0), cells were induced to differentiate in DMEM containing 10% FBS, 1 μg/ml insulin, 1 μM dexamethasone, and 0.5 mM 3-isobutyl-1-methylxanthine. 2 days post-differentiation (day 2), the medium was replaced with DMEM containing 1 μg/ml insulin and 10% FBS. Over the next 12 days, the medium was replaced every other day with a new one (DMEM containing 1 μg/ml insulin and 10% FBS). A DNA methyltransferase inhibitor, 5-AZA, was added at 5 μM whenever the medium was replaced every other day. The adenovirus infection and siRNA transfection procedures are shown in brief in Fig. 4*A*. An adenovirus designed to overexpress rat *St6gal1* (63) or control vector (LacZ) was added to the culture medium twice (days 0 and 2). For knockdown of integrin-β1, cells on a 6-cm dish were transfected with 80 pmol of siRNA using 8 μl of Lipofectamine 2000 (Life Technologies) 2 days post-confluence (day 0). Seven days after differentiation (day 7), total RNA and whole cell lysates were collected. Cells were collected and lysed with TBS containing 1% Triton X-100, a protease inhibitor mixture, and phosphatase inhibitors (Roche Applied Science) and subjected to protein analysis.

RNA Extraction, Reverse Transcription, and Real-time PCR—Total RNA from cultured cells or mouse VATs was extracted using TRI Reagent (Molecular Research Center, Inc.) according to the protocol of the manufacturer. Total RNA (1 μg) was reverse-transcribed using Superscript III (Life Technologies). For real-time PCR, cDNA was mixed with TaqMan Universal PCR Master Mix (Life Technologies) and amplified using an ABI Prism 7900HT. mRNA levels were normalized to corresponding *Gapdh* or rRNA levels.

Methylation-specific PCR Analysis—Genomic DNA was extracted from differentiated (14 days) or undifferentiated (0 day) 3T3-L1 cells using a Mammalian Genomic DNA Miniprep Kit (Sigma) according to the instructions of the manufacturer. Bisulfite treatment was performed with an innuCONVERT Bisulfite Basic Kit (Analytikjena). A genomic region in the CpG island of the *St6gal1* promoter was amplified by PCR (Epitaq HS, Takara) using two primer sets designed for either methylated or unmethylated CpGs. The primers were as follows: methylated, 5′-CGTTAGTTTGGGTTGGGGAGTC-3′ (forward) and 5′-CCCCTACACTCCTTCTTCAAAC-3′ (reverse); unmethylated, 5′-TGTTAGTTTGGGTTGGGGAGTT-3′ (forward) and 5′-CCCCTACACTCCTTCTTCAAAC-3′ (reverse).

Cell Proliferation Assay—3T3-L1 cells (preadipocytes) were infected with *St6gal1* ($n = 6$) or control vector (LacZ, $n = 6$) on day 0, and cell proliferation was assayed at each time point (24 and 48 h) using alamarBlue (68). Briefly, 3T3-L1 cells were seeded at 1×10^4 cells/well on a 96-well plate. After each incubation at 37 °C, a 1/10 volume of alamarBlue solution (Thermo Fisher Scientific) was directly added to the culture medium. After 3-h incubation at 37 °C, absorbance at 570 nm was measured. Values are shown relative to those of the cells on day 0.

Western and Lectin Blots—Proteins were separated by 5–20% gradient SDS-PAGE using the Laemmli buffer system and then transferred to nitrocellulose membranes. After blocking with 5% nonfat dry milk in TBS containing 0.05% Tween 20 (or blocking with TBS containing 0.1% Tween 20 for the lectin blot), the membranes were incubated with primary antibodies or biotinylated lectin (diluted with the blocking buffer), followed by HRP-conjugated secondary antibodies or HRP-conjugated streptavidin (Vectastain ABC Standard Kit). Proteins were detected with Western Lightning ECL Pro (PerkinElmer Life Sciences) using an ImageQuant LAS-4000mini (GE Healthcare).

SSA Lectin Precipitation—Mouse VAT lysates (300 μg of protein in 500 μl of TBS containing 1% Triton X-100, a protease inhibitor mixture, and phosphatase inhibitors (Roche Applied Science)) were incubated with 30 μl of SSA-agarose (Honen Co.) for 16 h with gentle shaking at 4 °C. The precipitates were washed four times with PBS and then eluted by boiling with SDS sample buffer. The precipitated proteins were separated by SDS-PAGE, stained with silver or transferred to nitrocellulose, and then probed with an anti-integrin-β1.

LC-MS/MS Analysis for Identification of Sialylated Proteins—The gel band that was reduced in HFD VATs was precipitated with SSA lectin from CON VATs (120–130 kDa), excised, and cut into small pieces. After washing and destaining the gel pieces, cysteine residues were reduced by DTT and alkylated with iodoacetamide. Proteins were digested with modified trypsin, and the resulting peptides were subjected to LC/MS-MS. LC/MS-MS analysis was performed using an Advance Nano LC (Bruker-Michrom, Auburn, CA) and LTQ linear ion trap mass spectrometer (Thermo Fisher Scientific, Inc., San Jose, CA) equipped with a NANO HPLC capillary column C18 (0.075-mm inner diameter × 150-mm length, 3-mm particle size, Nikkyo Technos, Tokyo, Japan) using a linear gradient (25 min, 5–35% CH_3CN/0.1% formic acid) at a flow rate of 300 nl/min. The resulting MS and MS-MS data were searched against the Swiss-Prot database using MASCOT software (Matrix Science, London, UK).

Immunofluorescence Staining—For histochemical analysis, VATs were fixed with paraformaldehyde, paraffin-embedded, sectioned at a thickness of 5 μm, and stained with biotinylated SSA lectin or DAPI. Briefly, VAT sections were incubated with 0.3% hydrogen peroxide in methanol and treated with the blocking solutions supplied in a tyramide signal amplification kit (TSA Biotin System, PerkinElmer Life Sciences), followed by incubation with biotinylated SSA lectin (overnight at 4 °C) and Alexa 488-labeled streptavidin (30 min at room temperature). DAPI was used for counterstaining. Fluorescence was visualized using an Olympus FV-1000 confocal microscope, and data acquisition and quantification of intensities were carried out using FV10-ASW ver.1.7 software (Olympus).

Author Contributions—T. K. and Y. K. conceived the idea for the project. T. K., Y. K., and S. K. designed the experiments. T. K. conducted most of the experiments, prepared figures, and wrote a draft manuscript. T. K., Y. K., S. K., and N. T. revised the paper. All authors interpreted the results, commented on the manuscript, and approved submission of the manuscript.

Acknowledgments—We thank Dr. Yuriko Tachida, Rie Imamaki, Reiko Fujinawa, Ritsuko Oka, Keiko Sato, and Kanoko Sakuda (RIKEN GRC) for technical help. We thank the Support Unit for Bio-Material Analysis, RIKEN BSI Research Resources Center, for technical help with LC/MS-MS analysis. We also thank Dr. Jamey D. Marth for providing the St6gal1 knockout mice and Dr. Ryoji Nagai for technical advice regarding 3T3-L1 cell culture.

References

1. Rosen, E. D., and Spiegelman, B. M. (2006) Adipocytes as regulators of energy balance and glucose homeostasis. *Nature* **444,** 847–853
2. Matsuzawa, Y., Funahashi, T., and Nakamura, T. (1999) Molecular mechanism of metabolic syndrome X: contribution of adipocytokines adipocyte-derived bioactive substances. *Ann. N.Y. Acad. Sci.* **892,** 146–154
3. Berg, A. H., Combs, T. P., and Scherer, P. E. (2002) ACRP30/adiponectin: an adipokine regulating glucose and lipid metabolism. *Trends Endocrinol. Metab.* **13,** 84–89
4. Ouchi, N., Kihara, S., Arita, Y., Maeda, K., Kuriyama, H., Okamoto, Y., Hotta, K., Nishida, M., Takahashi, M., Nakamura, T., Yamashita, S., Funahashi, T., and Matsuzawa, Y. (1999) Novel modulator for endothelial adhesion molecules: adipocyte-derived plasma protein adiponectin. *Circulation* **100,** 2473–2476
5. Mito, N., Yoshino, H., Hosoda, T., and Sato, K. (2004) Analysis of the effect of leptin on immune function in vivo using diet-induced obese mice. *J. Endocrinol.* **180,** 167–173
6. Fontana, L., Eagon, J. C., Trujillo, M. E., Scherer, P. E., and Klein, S. (2007) Visceral fat adipokine secretion is associated with systemic inflammation in obese humans. *Diabetes* **56,** 1010–1013
7. Kim, J. Y., van de Wall, E., Laplante, M., Azzara, A., Trujillo, M. E., Hofmann, S. M., Schraw, T., Durand, J. L., Li, H., Li, G., Jelicks, L. A., Mehler, M. F., Hui, D. Y., Deshaies, Y., Shulman, G. I., *et al.* (2007) Obesity-associated improvements in metabolic profile through expansion of adipose tissue. *J. Clin. Invest.* **117,** 2621–2637
8. Lissner, L., and Heitmann, B. L. (1995) Dietary fat and obesity: evidence from epidemiology. *Eur. J. Clin. Nutr.* **49,** 79–90
9. Lin, S., Thomas, T. C., Storlien, L. H., and Huang, X. F. (2000) Development of high fat diet-induced obesity and leptin resistance in C57Bl/6J mice. *Int. J. Obes. Relat. Metab. Disord.* **24,** 639–646
10. Shimomura, I., Funahashi, T., Takahashi, M., Maeda, K., Kotani, K., Nakamura, T., Yamashita, S., Miura, M., Fukuda, Y., Takemura, K., Tokunaga, K., and Matsuzawa, Y. (1996) Enhanced expression of PAI-1 in visceral fat: possible contributor to vascular disease in obesity. *Nat. Med.* **2,** 800–803
11. Patrick, C. W., Jr., and Wu, X. (2003) Integrin-mediated preadipocyte adhesion and migration on laminin-1. *Ann. Biomed. Eng.* **31,** 505–514
12. Kawaguchi, N., Sundberg, C., Kveiborg, M., Moghadaszadeh, B., Asmar, M., Dietrich, N., Thodeti, C. K., Nielsen, F. C., Möller, P., Mercurio, A. M., Albrechtsen, R., and Wewer, U. M. (2003) ADAM12 induces actin cytoskeleton and extracellular matrix reorganization during early adipocyte differentiation by regulating β1 integrin function. *J. Cell Sci.* **116,** 3893–3904
13. Moremen, K. W., Tiemeyer, M., and Nairn, A. V. (2012) Vertebrate protein glycosylation: diversity, synthesis and function. *Nat. Rev. Mol. Cell Biol.* **13,** 448–462
14. Ohtsubo, K., and Marth, J. D. (2006) Glycosylation in cellular mechanisms of health and disease. *Cell* **126,** 855–867
15. Taniguchi, N., Honke, K., Fukuda, M., Narimatsu, H., Yamaguchi, Y., and Angata, T. (2014) *Handbook of Glycosyltransferases and Related Genes*, Springer
16. Varki, A. C. R., Esko, J. D., Freeze, H. H., Stanley, P., Bertozzi, C. R., Hart, G. W., and Etzler, M. E. (2009) *Essentials of Glycobiology*, 2nd Ed., Cold Spring Harbor, New York
17. Rellier, N., Ruggiero-Lopez, D., Lecomte, M., Lagarde, M., and Wiernsperger, N. (1999) *In vitro* and *in vivo* alterations of enzymatic glycosylation in diabetes. *Life Sci.* **64,** 1571–1583
18. Lefebvre, T., Dehennaut, V., Guinez, C., Olivier, S., Drougat, L., Mir, A. M., Mortuaire, M., Vercoutter-Edouart, A. S., and Michalski, J. C. (2010) Dysregulation of the nutrient/stress sensor *O*-GlcNAcylation is involved in the etiology of cardiovascular disorders, type-2 diabetes and Alzheimer's disease. *Biochim. Biophys. Acta* **1800,** 67–79
19. Kabayama, K., Sato, T., Saito, K., Loberto, N., Prinetti, A., Sonnino, S., Kinjo, M., Igarashi, Y., and Inokuchi, J. (2007) Dissociation of the insulin receptor and caveolin-1 complex by ganglioside GM3 in the state of insulin resistance. *Proc. Natl. Acad. Sci. U.S.A.* **104,** 13678–13683
20. Lipina, C., and Hundal, H. S. (2015) Ganglioside GM3 as a gatekeeper of obesity-associated insulin resistance: evidence and mechanisms. *FEBS Lett.* **589,** 3221–3227
21. Ohtsubo, K., Chen, M. Z., Olefsky, J. M., and Marth, J. D. (2011) Pathway to diabetes through attenuation of pancreatic β cell glycosylation and glucose transport. *Nat. Med.* **17,** 1067–1075
22. Wang, X., Inoue, S., Gu, J., Miyoshi, E., Noda, K., Li, W., Mizuno-Horikawa, Y., Nakano, M., Asahi, M., Takahashi, M., Uozumi, N., Ihara, S., Lee, S. H., Ikeda, Y., Yamaguchi, Y., *et al.* (2005) Dysregulation of TGF-β1 receptor activation leads to abnormal lung development and emphysema-like phenotype in core fucose-deficient mice. *Proc. Natl. Acad. Sci. U.S.A.* **102,** 15791–15796
23. Li, X., Molina, H., Huang, H., Zhang, Y. Y., Liu, M., Qian, S. W., Slawson, C., Dias, W. B., Pandey, A., Hart, G. W., Lane, M. D., and Tang, Q. Q. (2009) *O*-linked *N*-acetylglucosamine modification on CCAAT enhancer-binding protein β: role during adipocyte differentiation. *J. Biol. Chem.* **284,** 19248–19254
24. Zaarour, N., Berenguer, M., Le Marchand-Brustel, Y., and Govers, R. (2012) Deciphering the role of GLUT4 *N*-glycosylation in adipocyte and muscle cell models. *Biochem. J.* **445,** 265–273
25. Vosseller, K., Wells, L., Lane, M. D., and Hart, G. W. (2002) Elevated nucleocytoplasmic glycosylation by *O*-GlcNAc results in insulin resistance associated with defects in Akt activation in 3T3-L1 adipocytes. *Proc. Natl. Acad. Sci. U.S.A.* **99,** 5313–5318
26. Haga, Y., Ishii, K., and Suzuki, T. (2011) *N*-glycosylation is critical for the stability and intracellular trafficking of glucose transporter GLUT4. *J. Biol. Chem.* **286,** 31320–31327
27. Yamauchi, T., Kamon, J., Waki, H., Terauchi, Y., Kubota, N., Hara, K., Mori, Y., Ide, T., Murakami, K., Tsuboyama-Kasaoka, N., Ezaki, O., Akanuma, Y., Gavrilova, O., Vinson, C., Reitman, M. L., *et al.* (2001) The fat-derived hormone adiponectin reverses insulin resistance associated with both lipoatrophy and obesity. *Nat. Med.* **7,** 941–946
28. Mito, N., Hosoda, T., Kato, C., and Sato, K. (2000) Change of cytokine balance in diet-induced obese mice. *Metabolism* **49,** 1295–1300
29. Nairn, A. V., York, W. S., Harris, K., Hall, E. M., Pierce, J. M., and Moremen, K. W. (2008) Regulation of glycan structures in animal tissues: transcript profiling of glycan-related genes. *J. Biol. Chem.* **283,** 17298–17313
30. Shibuya, N., Tazaki, K., Song, Z. W., Tarr, G. E., Goldstein, I. J., and Peumans, W. J. (1989) A comparative study of bark lectins from three elderberry (*Sambucus*) species. *J. Biochem.* **106,** 1098–1103
31. Hoffmann, L. S., Etzrodt, J., Willkomm, L., Sanyal, A., Scheja, L., Fischer, A. W., Stasch, J.-P., Bloch, W., Friebe, A., Heeren, J., and Pfeifer, A. (2015) Stimulation of soluble guanylyl cyclase protects against obesity by recruiting brown adipose tissue. *Nat. Commun.* **6,** 7235
32. Geurts, L., Everard, A., Van Hul, M., Essaghir, A., Duparc, T., Matamoros, S., Plovier, H., Castel, J., Denis, R. G., Bergiers, M., Druart, C., Alhouayek, M., Delzenne, N. M., Muccioli, G. G., Demoulin, J. B., *et al.* (2015) Adipose tissue NAPE-PLD controls fat mass development by altering the browning process and gut microbiota. *Nat. Commun.* **6,** 6495
33. Spiegelman, B. M., and Ginty, C. A. (1983) Fibronectin modulation of cell shape and lipogenic gene expression in 3T3-adipocytes. *Cell* **35,** 657–666
34. Wang, Y., Zhao, L., Smas, C., and Sul, H. S. (2010) Pref-1 interacts with fibronectin to inhibit adipocyte differentiation. *Mol. Cell Biol.* **30,** 3480–3492
35. Liu, J., DeYoung, S. M., Zhang, M., Zhang, M., Cheng, A., and Saltiel, A. R. (2005) Changes in integrin expression during adipocyte differentiation. *Cell Metab.* **2,** 165–177
36. Lin, T. H., Aplin, A. E., Shen, Y., Chen, Q., Schaller, M., Romer, L., Aukhil, I., and Juliano, R. L. (1997) Integrin-mediated activation of MAP kinase is

independent of FAK: evidence for dual integrin signaling pathways in fibroblasts. *J. Cell Biol.* **136,** 1385–1395
37. Martin, K. H., Slack, J. K., Boerner, S. A., Martin, C. C., and Parsons, J. T. (2002) Integrin connections map: to infinity and beyond. *Science* **296,** 1652–1653
38. Farmer, S. R. (2006) Transcriptional control of adipocyte formation. *Cell Metab.* **4,** 263–273
39. Rosen, E. D., and Spiegelman, B. M. (2000) Molecular regulation of adipogenesis. *Annu. Rev. Cell Dev. Biol.* **16,** 145–171
40. Londoño Gentile, T., Lu, C., Lodato, P. M., Tse, S., Olejniczak, S. H., Witze, E. S., Thompson, C. B., and Wellen, K. E. (2013) DNMT1 is regulated by ATP-citrate lyase and maintains methylation patterns during adipocyte differentiation. *Mol. Cell Biol.* **33,** 3864–3878
41. Boqué, N., de la Iglesia, R., de la Garza, A. L., Milagro, F. I., Olivares, M., Bañuelos, O., Soria, A. C., Rodríguez-Sánchez, S., Martínez, J. A., and Campión, J. (2013) Prevention of diet-induced obesity by apple polyphenols in Wistar rats through regulation of adipocyte gene expression and DNA methylation patterns. *Mol. Nutr. Food Res.* **57,** 1473–1478
42. Farnier, C., Krief, S., Blache, M., Diot-Dupuy, F., Mory, G., Ferre, P., and Bazin, R. (2003) Adipocyte functions are modulated by cell size change: potential involvement of an integrin/ERK signalling pathway. *Int. J. Obes. Relat. Metab. Disord.* **27,** 1178–1186
43. Whitfield, M. L., George, L. K., Grant, G. D., and Perou, C. M. (2006) Common markers of proliferation. *Nat. Rev. Cancer* **6,** 99–106
44. Semel, A. C., Seales, E. C., Singhal, A., Eklund, E. A., Colley, K. J., and Bellis, S. L. (2002) Hyposialylation of integrins stimulates the activity of myeloid fibronectin receptors. *J. Biol. Chem.* **277,** 32830–32836
45. Seales, E. C., Shaikh, F. M., Woodard-Grice, A. V., Aggarwal, P., McBrayer, A. C., Hennessy, K. M., and Bellis, S. L. (2005) A protein kinase C/Ras/ERK signaling pathway activates myeloid fibronectin receptors by altering beta1 integrin sialylation. *J. Biol. Chem.* **280,** 37610–37615
46. Isaji, T., Im, S., Gu, W., Wang, Y., Hang, Q., Lu, J., Fukuda, T., Hashii, N., Takakura, D., Kawasaki, N., Miyoshi, H., and Gu, J. (2014) An oncogenic protein Golgi phosphoprotein 3 up-regulates cell migration via sialylation. *J. Biol. Chem.* **289,** 20694–20705
47. Woodard-Grice, A. V., McBrayer, A. C., Wakefield, J. K., Zhuo, Y., and Bellis, S. L. (2008) Proteolytic shedding of ST6Gal-I by BACE1 regulates the glycosylation and function of α4β1 integrins. *J. Biol. Chem.* **283,** 26364–26373
48. Lu, J., Isaji, T., Im, S., Fukuda, T., Kameyama, A., and Gu, J. (2016) Expression of *N*-acetylglucosaminyltransferase III suppresses α2,3 sialylation, and its distinctive functions in cell migration are attributed to α2,6-sialylation levels. *J. Biol. Chem.* **291,** 5708–5720
49. Hedlund, M., Ng, E., Varki, A., and Varki, N. M. (2008) α2–6-Linked sialic acids on *N*-glycans modulate carcinoma differentiation *in vivo*. *Cancer Res.* **68,** 388–394
50. Lu, J., and Gu, J. (2015) Significance of β-galactoside α2,6 sialyltranferase 1 in cancers. *Molecules* **20,** 7509–7527
51. Fuentes, P., Acuña, M. J., Cifuentes, M., and Rojas, C. V. (2010) The anti-adipogenic effect of angiotensin II on human preadipose cells involves ERK1,2 activation and PPARG phosphorylation. *J. Endocrinol.* **206,** 75–83
52. Scott, R. E., Florine, D. L., Wille, J. J., Jr, and Yun, K. (1982) Coupling of growth arrest and differentiation at a distinct state in the G_1 phase of the cell cycle: GD. *Proc. Natl. Acad. Sci. U.S.A.* **79,** 845–849
53. Zhang, J. W., Tang, Q. Q., Vinson, C., and Lane, M. D. (2004) Dominant-negative C/EBP disrupts mitotic clonal expansion and differentiation of 3T3-L1 preadipocytes. *Proc. Natl. Acad. Sci. U.S.A.* **101,** 43–47
54. Lauc, G., Vojta, A., and Zoldoš, V. (2014) Epigenetic regulation of glycosylation is the quantum mechanics of biology. *Biochim. Biophys. Acta* **1840,** 65–70
55. Kizuka, Y., Kitazume, S., Okahara, K., Villagra, A., Sotomayor, E. M., and Taniguchi, N. (2014) Epigenetic regulation of a brain-specific glycosyltransferase *N*-acetylglucosaminyltransferase-IX (GnT-IX) by specific chromatin modifiers. *J. Biol. Chem.* **289,** 11253–11261
56. Kawamura, Y. I., Toyota, M., Kawashima, R., Hagiwara, T., Suzuki, H., Imai, K., Shinomura, Y., Tokino, T., Kannagi, R., and Dohi, T. (2008) DNA hypermethylation contributes to incomplete synthesis of carbohydrate determinants in gastrointestinal cancer. *Gastroenterology* **135,** 142–151.e3
57. Kizuka, Y., and Taniguchi, N. (2016) Enzymes for *N*-glycan branching and their genetic and nongenetic regulation in cancer. *Biomolecules* **6,** 25
58. Antony, P., Rose, M., Heidenreich, A., Knüchel, R., Gaisa, N. T., and Dahl, E. (2014) Epigenetic inactivation of ST6GAL1 in human bladder cancer. *BMC Cancer* **14,** 901
59. Minami, A., Shimono, Y., Mizutani, K., Nobutani, K., Momose, K., Azuma, T., and Takai, Y. (2013) Reduction of the ST6 β-galactosamide α-2,6-sialyltransferase 1 (ST6GAL1)-catalyzed sialylation of nectin-like molecule 2/cell adhesion molecule 1 and enhancement of ErbB2/ErbB3 signaling by microRNA-199a. *J. Biol. Chem.* **288,** 11845–11853
60. Kroes, R. A., and Moskal, J. R. (2016) The role of DNA methylation in ST6Gal1 expression in gliomas. *Glycobiology* **26,** 1271–1283
61. Hennet, T., Chui, D., Paulson, J. C., and Marth, J. D. (1998) Immune regulation by the ST6Gal sialyltransferase. *Proc. Natl. Acad. Sci. U.S.A.* **95,** 4504–4509
62. Marino, J. H., Tan, C., Davis, B., Han, E. S., Hickey, M., Naukam, R., Taylor, A., Miller, K. S., Van De Wiele, C. J., and Teague, T. K. (2008) Disruption of thymopoiesis in ST6Gal I-deficient mice. *Glycobiology* **18,** 719–726
63. Kitazume, S., Imamaki, R., Ogawa, K., Komi, Y., Futakawa, S., Kojima, S., Hashimoto, Y., Marth, J. D., Paulson, J. C., and Taniguchi, N. (2010) α2,6-sialic acid on platelet endothelial cell adhesion molecule (PECAM) regulates its homophilic interactions and downstream antiapoptotic signaling. *J. Biol. Chem.* **285,** 6515–6521
64. Shabana Ullah Shahid, S., Wah Li, K., Acharya, J., Cooper, J. A., Hasnain, S., and Humphries, S. E. (2016) Effect of six type II diabetes susceptibility loci and an FTO variant on obesity in Pakistani subjects. *Eur. J. Hum. Genet.* **24,** 903–910
65. Kooner, J. S., Saleheen, D., Sim, X., Sehmi, J., Zhang, W., Frossard, P., Been, L. F., Chia, K. S., Dimas, A. S., Hassanali, N., Jafar, T., Jowett, J. B., Li, X., Radha, V., Rees, S. D., *et al.* (2011) Genome-wide association study in individuals of South Asian ancestry identifies six new type 2 diabetes susceptibility loci. *Nat. Genet.* **43,** 984–989
66. Kitazume, S., Oka, R., Ogawa, K., Futakawa, S., Hagiwara, Y., Takikawa, H., Kato, M., Kasahara, A., Miyoshi, E., Taniguchi, N., and Hashimoto, Y. (2009) Molecular insights into β-galactoside α2,6-sialyltransferase secretion *in vivo*. *Glycobiology* **19,** 479–487
67. Kizuka, Y., Nakano, M., Miura, Y., and Taniguchi, N. (2016) Epigenetic regulation of neural *N*-glycomics. *Proteomics* **16,** 2854–2863
68. Ahmed, S. A., Gogal, R. M., Jr, and Walsh, J. E. (1994) A new rapid and simple non-radioactive assay to monitor and determine the proliferation of lymphocytes: an alternative to [3H]thymidine incorporation assay. *J. Immunol. Methods* **170,** 211–224